

Seasonal climate summary southern hemisphere (winter 2009): a developing El Niño and an exceptionally warm winter for much of Australia

Dörte Jakob

National Climate Centre, Bureau of Meteorology, Australia

(Manuscript received February 2010; revised March 2010)

Southern hemisphere circulation patterns and associated anomalies for the austral winter 2009 are reviewed, with emphasis given to the Pacific Basin climate indices and Australian rainfall and temperature patterns.

Sea-surface temperatures remained significantly higher than the long-term average across most of the tropical Pacific Ocean in winter, exceeding El Niño thresholds from west of the date-line to the South American coast. Subsurface waters cooled through July and August, but a large volume of the subsurface still remained significantly warmer than the long-term average. The SOI was near-neutral for the season, not indicating an El Niño state. Trade winds were generally weaker than normal across the tropical Pacific. Although cloudiness near the date-line increased, it did not show a strong trend towards El Niño-like values.

The season was exceptionally warm over much of Australia. Average maximum temperatures over the country were the highest on record, while seasonal mean temperatures fell only just short of the 1996 record. It was also a rather dry season over much of the continent, particularly the north and east.

Introduction

This summary reviews southern hemisphere climate patterns acting around Australia and the southern hemisphere for the austral winter (June to August) 2009. Particular attention is given to the Australasian and the Pacific regions. The main sources of information used for this summary were the analyses prepared by the Bureau of Meteorology and the Centre for Australian Weather and Climate Research (CAWCR).

ENSO and Pacific Basin climate indices

The Troup Southern Oscillation Index (SOI)¹

The SOI for the period January 2005 to August 2009 is shown in Fig. 1, together with a five-month weighted mo-

ving average. The SOI is derived from the mean sea-level pressure (MSLP) at both Darwin and Tahiti, and sustained values can be used as an indicator of El Niño-Southern Oscillation (ENSO) events.

The SOI fluctuated around a falling trend in autumn 2009, consistent with a return from La Niña to more neutral conditions (Chandler 2009). SOI values for the winter marked this as a season in transition, with a value of -2.3 for June which increased to $+1.6$ for July and then decreased to -5.0 in August. The MSLP values for both Darwin and Tahiti were close to the long-term average: monthly anomalies based on the period 1933-1992 for the three winter months (June to August) at Darwin stayed very close to zero ($+0.2$, 0.0 and $+0.1$ hPa, respectively), with the corresponding monthly anomalies at Tahiti being -0.1 , $+0.3$ and -0.7 hPa.

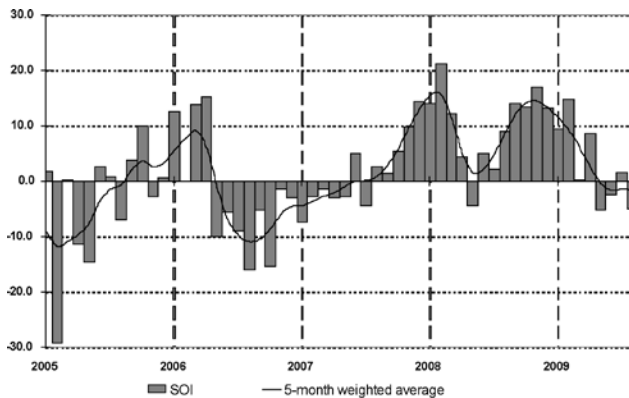
Corresponding author address: Dörte Jakob, National Climate Centre, Bureau of Meteorology, GPO Box 1289, Melbourne VIC 3001. Email: D.Jakob@bom.gov.au

¹ The Troup SOI (Troup 1965) used in this article is ten times the standardised monthly anomaly of the difference in MSLP between Tahiti and Darwin. The standardisation calculation is based on a sixty-year climatology (1933-1992). The Tahiti MSLP data are provided by Météo France interregional direction for French Polynesia. Monthly SOI data, together with contributing monthly MSLP data from Tahiti and Darwin, are obtained from <http://www.bom.gov.au/climate/current/soihtm1.shtml>.

Multivariate ENSO index

The US Climate Diagnostics Center's Multivariate ENSO Index (MEI) is derived from a number of atmospheric and oceanic parameters typically associated with ENSO (Climate Diagnostics Center 2009a and 2009b), and calculated as a

Fig. 1 Southern Oscillation Index from January 2005 to August 2009, together with a five-month binomially weighted moving average. Means and standard deviations used in the computation of the SOI are based on the period 1933-1992.



bimonthly value (Wolter and Timlin 1993, 1998). The index is a standardised anomaly index, with positive (negative) values indicative of El Niño (La Niña).

The MEI value rose from +0.90 for June/July to +0.98 for July/August, the highest value since the December 2006/January 2007 value (+0.99). The rank of the MEI value for July/August was 51 out of 60 and therefore above the 80th percentile for MEI rankings for this season, indicating moderate El Niño conditions based on the MEI.

Outgoing long-wave radiation

Outgoing long-wave radiation (OLR) over the equatorial Pacific is a good measure of tropical deep convection, with increases in OLR indicating decreases in convection and vice versa. Convection in the equatorial region centred about the date-line is sensitive to changes in the Walker Circulation. Studies have shown that during El Niño events, OLR is generally reduced (i.e. convection is generally enhanced) along the equator, particularly near and east of the date-line. During La Niña events, OLR is often increased (i.e. convection is often suppressed) over the same region (Vincent et al. 1998).

The spatial pattern of seasonal OLR anomalies across the Asia/Pacific tropics for winter 2009 is shown in Fig. 2, while Fig. 3 shows the development of OLR anomalies in the vicinity of the date-line over time. In seasonally averaged terms, equatorial OLR anomalies near the date-line were fairly weak, being positive in June and August, and negative in July, while they were consistent with the end of a weak late-peaking La Niña event. Tropical convection remained suppressed over Indonesia (and extending into Australia) during August, consistent with the onset of a weak El Niño. However, convection remained near-normal over the near-equatorial Pacific.

Fig. 2 Anomalies of OLR for winter 2009 ($W m^{-2}$). Base period 1979 to 1998. The mapped region extends from 40°S to 40°N and 70°E to 180°E.

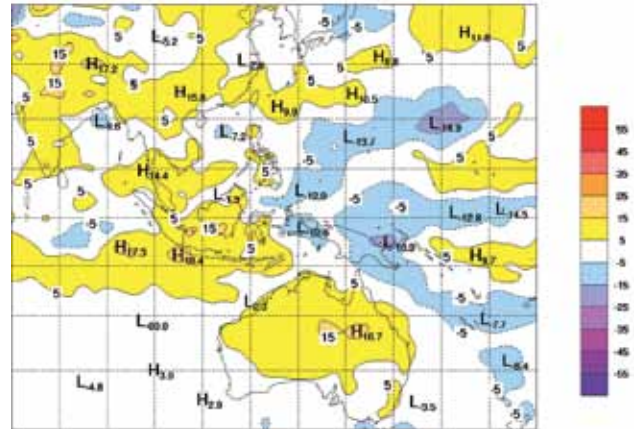
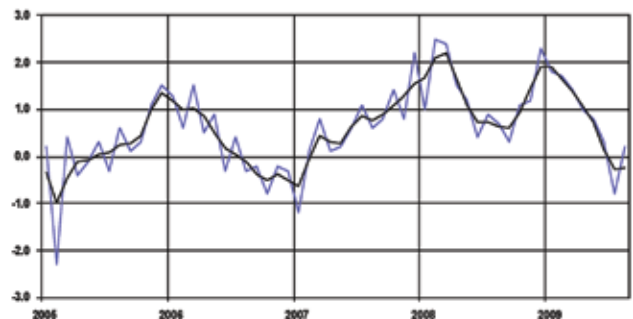


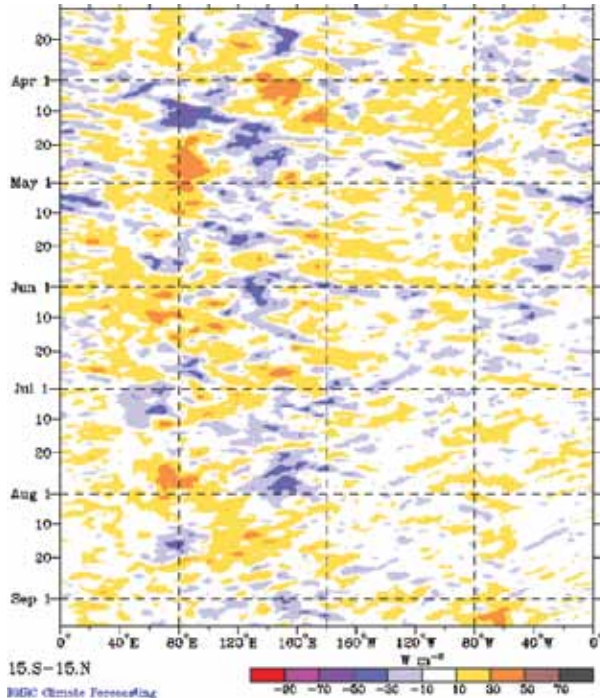
Fig. 3 Standardised anomaly of monthly OLR averaged over the area 5°S – 5°N and 160°E – 160°W, from January 2005 to August 2009, together with a three-month moving average. Negative (positive) anomalies indicate enhanced (reduced) convection and rainfall in the area. Anomalies are based on the 1979-1995 base period. After Climate Prediction Center (2009).



Madden-Julian Oscillation

The Madden-Julian Oscillation (MJO) is a tropical atmospheric anomaly which develops in the Indian Ocean and propagates eastwards into the Pacific Ocean (Donald et al. 2004). The MJO takes between 30 to 60 days to reach the western Pacific and has a frequency of six to twelve events per year (Donald et al. 2004). When the MJO is in an active phase, it is associated with increased tropical convection. The temporal evolution of tropical convection anomalies along the equator is shown in Fig. 4, covering the period March to September 2009. In June the MJO signal occupied phase six, seven, eight and one (Wheeler and Hendon 2004), which partly explains a break in the Indian monsoon. The MJO weakened in July which led to a recovery of the Indian monsoon. There was little MJO activity for most of August when convection remained near-normal over the near-equatorial Pacific.

Fig. 4 Time-longitude section of daily averaged OLR anomalies (11 March to 9 September 2009). The base period is 1979-2001.



Oceanic patterns

Sea-surface temperatures

Winter 2009 global sea-surface temperature (SST) anomalies, obtained from the US National Oceanic and Atmospheric Administration Optimum Interpolation analysis (Reynolds et al. 2002), are shown in Fig. 5. Positive (warm) anomalies are shown in red shades, and negative (cool) anomalies in blue shades. The equatorial Pacific rapidly transitioned from a neutral to a warm state from late autumn to early winter. The SST anomalies showed a warm tongue in the eastern Pacific Ocean that is typical for El Niño events. However, these temperature anomalies were not very strong and they were not accompanied by negative anomalies north and south of the warm tongue. Overall anomalies stayed the same for July and August, as indicated by the NINO indices, but became more fragmented in August and spread further to the west.

All three standard monthly NINO indices² were positive during winter 2009, and at levels that reflected the development of an El Niño event. The eastern equatorial Pacific NINO3 SST anomaly index went positive in April 2009 and remained positive through to the end of winter (monthly values of +0.82, +1.09 and +1.08°C), while the corresponding monthly

values for the central equatorial Pacific NINO3.4 index were +0.58, +0.87 and +0.82°C, with +0.62, +0.67 and +0.82°C for the western equatorial Pacific NINO4 index. The rise in all three NINO indices continued the warming trend that had been evident across most of the equatorial Pacific since autumn 2009. More importantly they signified the onset of a new El Niño event, even though the atmospheric indicators (e.g. the SOI and the OLR index) lagged behind.

The Dipole Mode Index (Saji et al. 1999) measures the difference in SST anomaly between the tropical west (50°E to 70°E and 10°S to 10°N) and east (90°E to 110°E and 10°S to 0°S) of the equatorial Indian Ocean; a positive phase often results in a decrease of rainfall over parts of central and southern Australia. The Indian Ocean was in a neutral phase during winter 2009. Anomalies during winter ranged from +0.6°C, mostly in early winter, to -0.6°C, with most of the weak negative anomalies occurring later in the season. Figure 5 shows positive anomalies for winter for both the west and the east pole of the IOD, but with slightly higher positive anomalies in the east. SSTs were slightly above average in winter around most of the Australian coastline, the major exception being off the southwest coast of Western Australia.

Subsurface ocean patterns

A Hovmöller diagram for the 20°C isotherm depth anomaly across the equator from January 2001 to August 2009, obtained from the Centre for Australian Weather and Climate Research (CAWCR), is shown in Fig. 6. The 20°C isotherm depth is generally situated close to the equatorial ocean thermocline, the region of greatest temperature gradient with depth and the boundary between the warm near-surface and cold deep ocean water. Positive anomalies correspond to the 20°C isotherm being deeper than average, and negative anomalies to it being shallower than average. Changes in the thermocline depth may act as a precursor to subsequent changes at the surface.

Figure 7 shows a cross-section of the equatorial Pacific temperature anomaly profile down to 400 metres for the months May to August 2009. Red shades indicate positive anomalies (downwelling), and blue shades negative anomalies (upwelling). In profile, the downwelling wave which initiated in summer is still evident. Regions of negative temperature anomalies are almost absent.

Positive anomalies dominated the subsurface in the equatorial Pacific. A Kelvin wave had progressed eastwards during autumn and reached the eastern boundary in winter, bringing warm water close to the surface which led to the warm signal observed in the SST anomalies (Fig. 5). Another Kelvin wave developed in late winter and propagated towards the east. Analogous to the development in SST anomalies, negative subsurface temperature anomalies had been rapidly replaced by positive anomalies in the central and eastern equatorial Pacific. These positive subsurface anomalies in the central and eastern Pacific gradually weakened during the season to a near neutral, but marginally warm, state by the end of August.

² NINO SST indices obtained from <ftp://ftp.cpc.ncep.noaa.gov/wd52dg/data/indices/ssoi/indices>, and NINO SST anomaly indices subsequently calculated with respect to the 1961-1990 period.

Fig. 5 Global anomalies of SST (°C) for winter 2009. The contour interval is 0.5°C and the base period is 1961-1990.

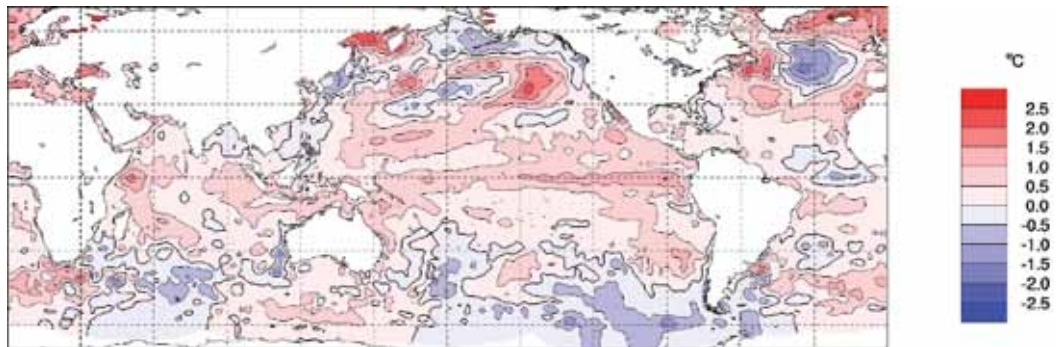
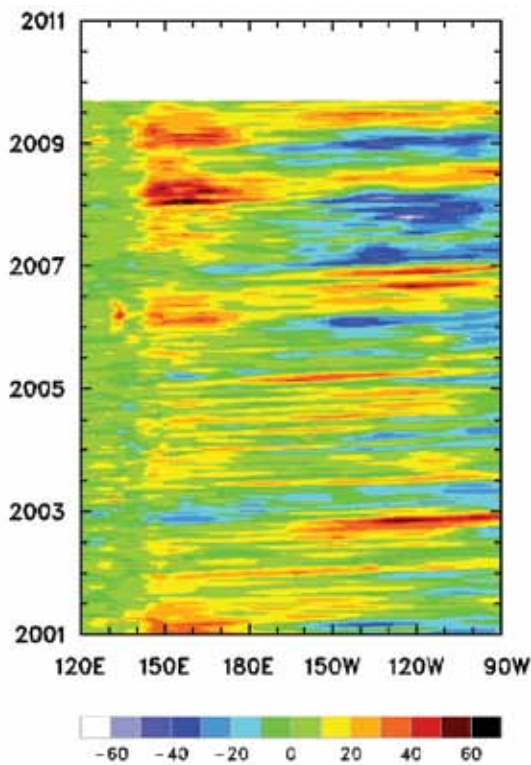


Fig. 6 Time-longitude section of the monthly anomalous depth of the 20°C isotherm at the equator from January 2001 to August 2009. The contour interval is 10m.



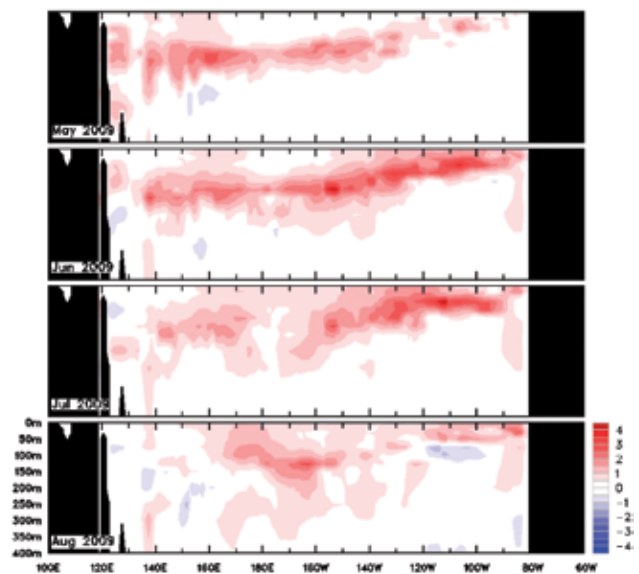
At this time (i.e. August), most coupled El Niño prediction models were continuing to forecast the intensification of the event, even though the only clear indicator at typical El Niño levels was the SST.

Atmospheric patterns

Surface analyses

The southern hemisphere winter 2009 MSLP pattern, computed from the Bureau of Meteorology's Global Assimilation and Prediction (GASP) model, is shown in Fig. 8, with the associated anomaly pattern shown in Fig. 9. These

Fig. 7 Four-month (May to August 2009) sequence of vertical temperature anomalies at the equator for the Pacific Ocean. The contour interval is 0.5°C.



anomalies are the difference from a 1979-2000 climatology obtained from the National Center for Environmental Prediction (NCEP) II Reanalysis data (Kanamitsu et al. 2002). The MSLP analysis has been computed using data from the 0000 UTC daily analyses of the GASP model. The MSLP anomaly field is not shown over areas of elevated topography (grey shading).

The MSLP showed a strong zonal pattern for the autumn season (Chandler 2009). For winter, there was a weak tendency towards a three-wave pattern, with troughs at around 115°E, 135°W and 30°W. Anomalous high pressure occurred over the southern Indian Ocean, but MSLP was close to average over inland Australia. A -5 hPa anomalous low located close to the South Australian coastline, southwest of Adelaide, was the strongest anomaly feature in the Australian region. It was associated with above average winter rainfall in Tasmania and across parts of the southern coastline.

Fig. 8 Southern hemisphere winter 2009 MSLP (hPa). The contour interval is 5 hPa.

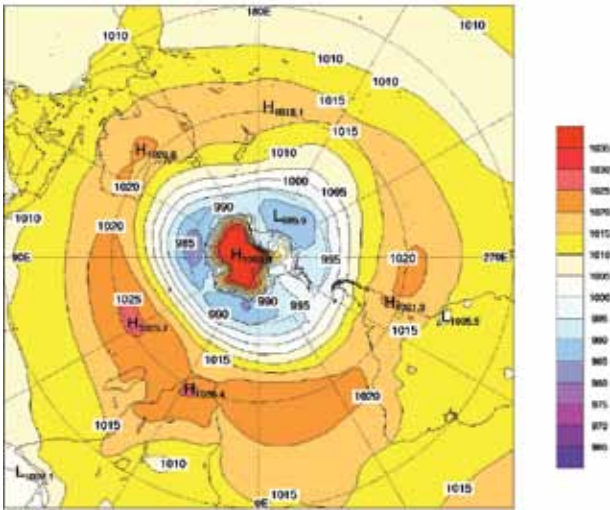


Fig. 9 Southern hemisphere winter 2009 MSLP anomalies (hPa). The contour interval is 2.5 hPa.

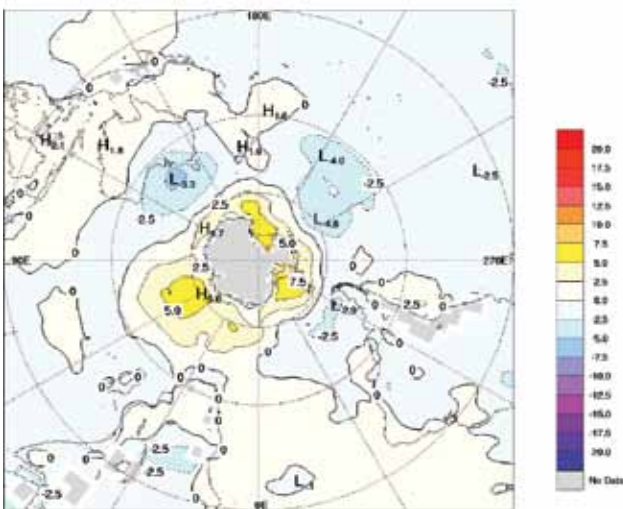


Fig. 10 Southern hemisphere winter 2009 500 hPa mean geopotential height (gpm). The contour interval is 100 gpm.

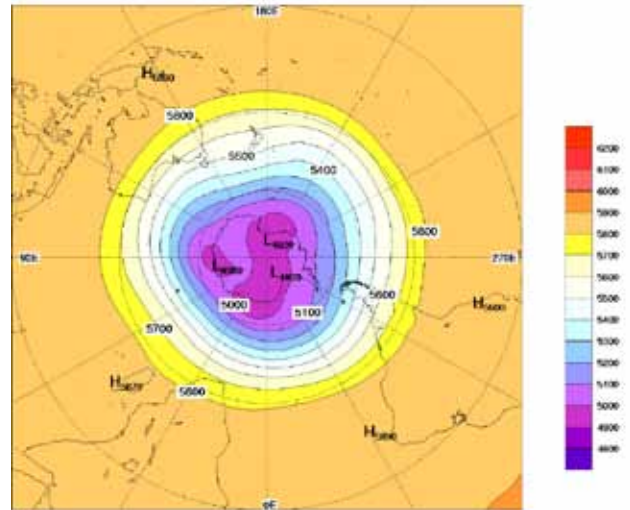
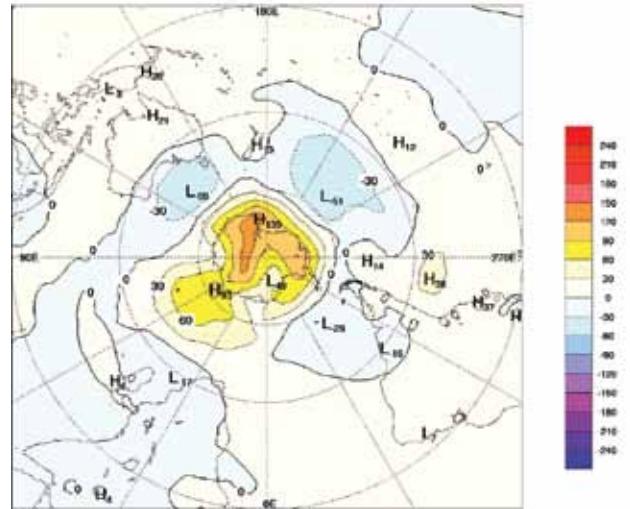


Fig. 11 Southern hemisphere winter 2009 500 hpa geopotential anomaly (gpm). The contour interval is 30 gpm.



The Southern Annular Mode (SAM) describes the periodic (10-day) oscillation of atmospheric pressure between polar and mid-latitude regions of the southern hemisphere. Positive phases of SAM describe increased mass over the extratropics, decreased mass over Antarctica and enhanced mid-latitude westerly flow that is contracted poleward. Conversely, negative phases of SAM describe increased mass over Antarctica, reduced mass over the extratropics and weakened meridional circulation that is expanded equatorward. The US Climate Prediction Center's standardised monthly SAM index³ (Climate Prediction Center 2009) remained in its negative phase for the winter months (-0.47, -1.23 and -0.69 for June, July and August

³This index is derived from daily 700 hPa height anomalies south of 20°S.

respectively). The winter seasonal average of this index is negatively correlated with winter rainfall across southern New South Wales, Victoria, Tasmania and the southwest coast of Western Australia between Albany and Geraldton. Above average rainfall was recorded only for some of these regions, notably for Tasmania which received very much above average rainfall (Fig. 16).

Mid-tropospheric analyses

The 500 hPa geopotential height (an indicator of the steering of surface synoptic systems) across the southern hemisphere is shown in Fig. 10, with the associated anomalies shown in Fig. 11. A comparison of Fig. 9 and Fig. 11 displays barotropic pressure anomalies throughout the southern hemisphere. The three-wave pattern noted in Fig. 8 can also be seen in Fig. 10.

Blocking

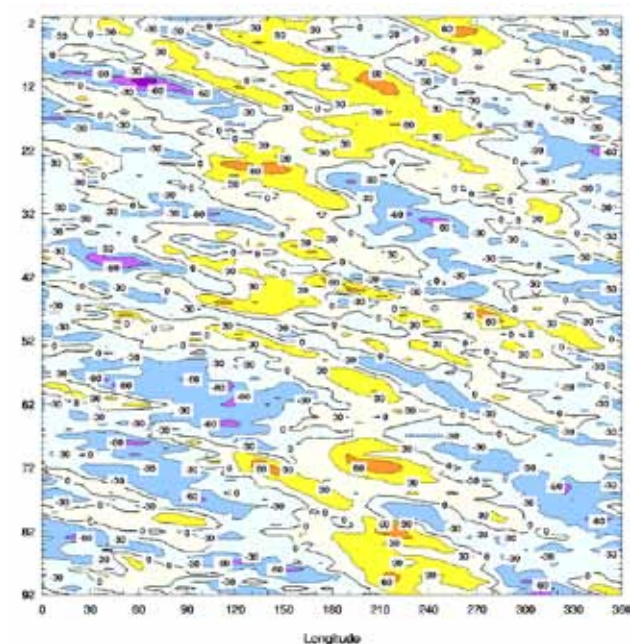
The time-longitude section of the daily southern hemisphere blocking index (BI)⁴ is shown in Fig. 12, with the start of the season at the top of the figure. This index is a measure of the strength of the zonal 500 hPa flow in mid-latitudes relative to that at lower and higher latitudes. Positive values of the blocking index are generally associated with a split in the mid-latitude westerly flow centred near 45°S and mid-latitude blocking activity.

In June, most blocking activity occurred in the band from about 100°E to 90°W, with positive anomalies dominating that period. In late winter blocking was confined to a narrower band (120°E to 90°W). Two blocking minima occurred around mid-June and early July at about 60°E. Fig. 13, which shows the seasonal index for each longitude, indicates that blocking for winter 2009 was very close to the long-term average across most longitudes.

Winds

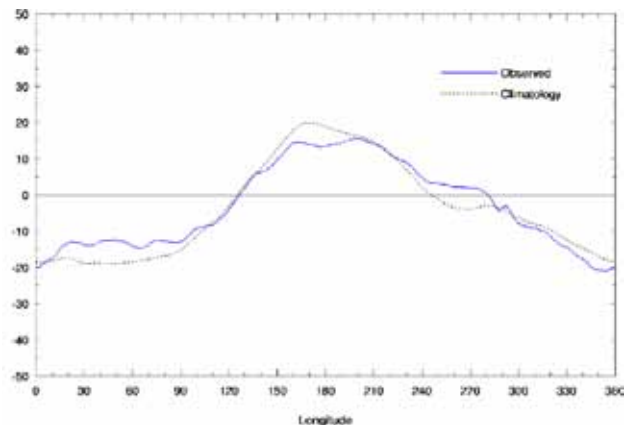
Winter 2009 low-level (850 hPa) and upper-level (200 hPa) wind anomalies (from the 22-year NCEP II climatology) are shown in Fig. 14(a) and Fig. 14(b) respectively. Isotach contours are at 5 m s⁻¹ intervals, and in Fig. 14(a), regions where the surface rises above the 850 hPa level are shaded in grey.

Fig. 12 Winter 2009 daily blocking index: time-longitude section. Day 1 is 1 June 2009. The horizontal axis shows the degrees east of the Greenwich meridian.



⁴ The blocking index is defined as $BI = 0.5[u_{25} + u_{30} - (u_{40} + 2u_{45} + u_{50}) + u_{55} + u_{60}]$ where u_x is the zonal (east-west) component of the 500 hPa wind at latitude x .

Fig. 13 Mean southern hemisphere blocking index for winter 2009 (solid line). The dashed line shows the corresponding long-term average.



In keeping with the ambiguous start to this potential El Niño, low-level zonal wind anomalies over the equatorial Pacific did not show a consistent trend during the season. However, in the seasonal mean they were westerly in character west of about 170°E and east of around 160°W – an indication for a developing El Niño event. These wind anomalies are reflected in the SST anomalies seen in Fig. 5. Low-level cyclonic anomalies affected southern regions of Australia, consistent with the negative MSLP anomaly in Fig. 9.

Upper-wind anomalies in the southern hemisphere locally reached 13.0 m s⁻¹ for winter 2009. These were situated in an area of westerly anomalies located over the central South Pacific, while another weaker band of northwesterly and westerly anomalies extended from the Indian Ocean to southern parts of Australia. In contrast at high latitudes, a band of easterly anomalies stretched from about 100°E to 90°W.

Australian region climate

Rainfall

Rainfall totals for winter are shown in Fig. 15, while the rainfall deciles for the same period are shown in Fig. 16. Rainfall deciles are calculated using all winters from 1900 to 2009.

Winter was a generally dry season away from the southern coast, with nationally averaged winter rainfall 23 per cent below average (27th lowest of 110 years). Northern and eastern areas were especially dry, with the Northern Territory (seasonally dry at this time of year) 84 per cent below average and Queensland 63 per cent below average. Rainfall totals were in decile 1 (i.e. below the 10th percentile) along the Queensland coast between Cooktown and Bundaberg, and extending inland along the Flinders Highway corridor from Townsville to Mount Isa (amounting to 39.5 per cent of the State). Most of far western Queensland, the Northern Territory, northeastern South Australia and the north of Western Australia received little or no rain for the season. There were also areas of decile 1 rainfall on the NSW-Queensland border around Goondiwindi, and on the NSW South Coast around Nowra.

Fig. 14(a) Global winter 2009 850 hPa vector wind anomalies (m s^{-1}). The contour interval is 5 m s^{-1} .

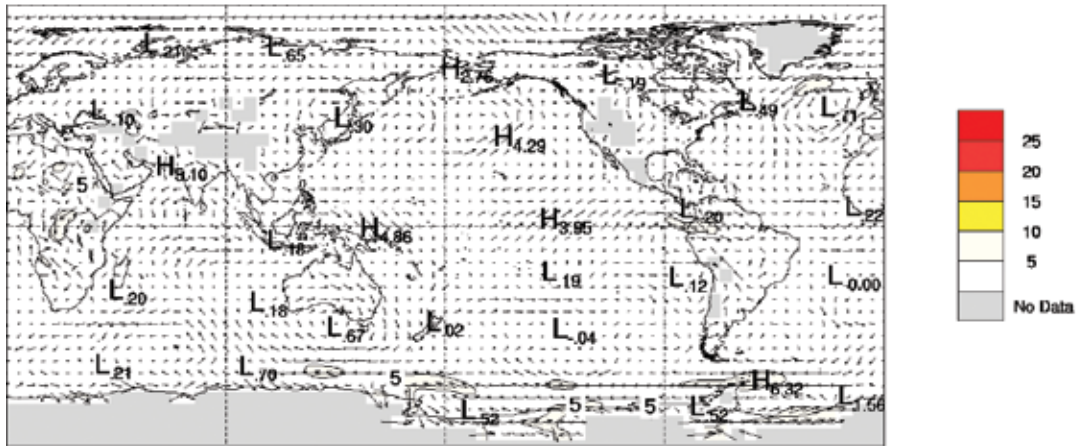


Fig. 14(b) Global winter 2009 200 hPa vector wind anomalies (m s^{-1}). The contour interval is 5 m s^{-1} .

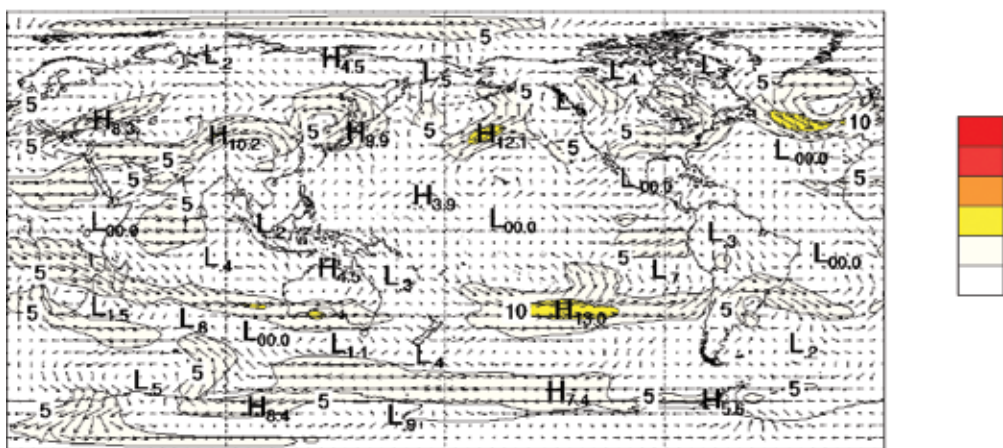


Fig. 15 Winter 2009 rainfall totals (mm) for Australia.

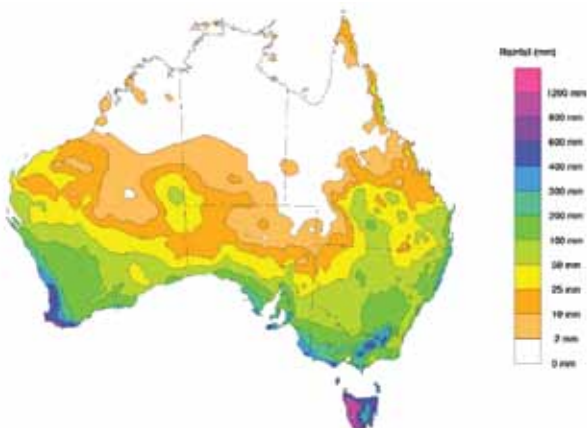


Fig. 16 Winter 2009 rainfall for Australia: decile ranges based on grid-point values over the winters 1900 to 2009.

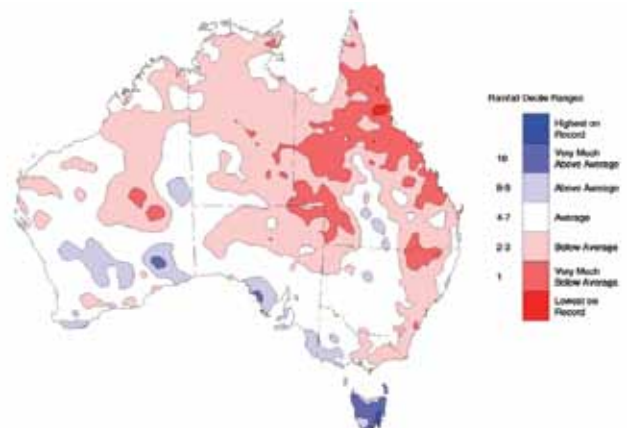


Table 1. Summary of seasonal rainfall ranks and extremes on a national and State basis for winter 2009.

	<i>Highest seasonal total (mm)</i>	<i>Lowest seasonal total (mm)</i>	<i>Highest 24 hour fall (mm)</i>	<i>Area-averaged rainfall (AAR) (mm)</i>	<i>Rank of AAR *</i>
Australia	1203 at Lake Margaret (Tas)	0 at numerous locations in WA, NT, Qld, SA	157 at Upper Springbrook (Qld), 22 June	49	27
WA	847 at Northcliffe	0 at numerous locations	82 at Sherlock, 12 June	51	43
NT	24 at Uluru Rangers	0 at numerous locations	23 at Point Fawcett, 9 June	3	20
SA	584 at Brookland Park	0 at numerous locations	53 at Mabenjo, 2 July	49	41
QLD	425 at Upper Springbrook	0 at numerous locations	157 at Upper Springbrook, 22 June	19	15
NSW	607 at Thredbo Village	0.8 at Fort Grey	148 at Upper Orara, 22 June	93	26
VIC	884 at Rocky Valley	54 at Pirlita	77 at Rocky Valley, 1 July	188	43
AS	1203 at Lake Margaret	201 at Melton Mowbray	143 at St. Marys, 13 August	656	107

* The rank goes from 1 (lowest) to 110 (highest) and is calculated over the years 1900 to 2009 inclusive.

In contrast, it was a very wet winter in Tasmania, ranking as the fourth wettest on record (49 per cent above average). Records were set on parts of the east coast between Swansea and Bruny Island. Most areas south of a St Helens-Queenstown line were in decile 10 (i.e. above the 90th percentile), as were parts of the northwest and Flinders Island. Whilst no part of the mainland was comparably wet, winter rainfall did match or exceed seasonal averages over most agricultural areas of South Australia, much of the western half of Victoria, and southwestern Western Australia west of a Geraldton-Bremer Bay line, as well as locally on the Mid-North Coast of New South Wales and around Charleville in Queensland.

Drought

At the end of winter 2009, 18 per cent of Australia was in serious rainfall deficiency (decile 1) for the six months ending in August 2009 (6.6 per cent in severe deficiency, i.e. below the 5th percentile). This comprised 34.8 per cent of the Northern Territory (16.5 per cent in severe deficiency), 25.5 per cent of Queensland (7.4 per cent in severe deficiency) and 15.0 per cent of Western Australia (5.7 per cent in severe deficiency). The next local temporal maxima in the national percentage area with serious rainfall deficiencies were at 20 months (6.6 per cent of Australia in serious deficiency for the 20 months ending August 2009) and at 27 months (10.4 per cent of Australia in serious deficiency for the 27 months ending August 2009).

Temperatures

Winter 2009 was exceptionally warm over much of Australia. August was particularly extreme; the national maximum temperature anomaly for the month was +3.20°C, the largest on record for any month, while the mean temperature anomaly of +2.47°C was an August record, and many site records were set. A special climate statement on the August and winter extremes is available from the Bureau's webpages (<http://www.bom.gov.au/climate/current/special-statements.shtml>).

Figure 17 shows maximum and minimum temperature anomalies for autumn, the corresponding deciles are shown in Fig. 18 and mean temperature deciles are shown in Fig. 19. Seasonal anomalies are calculated with respect to the 1961-1990 period using all stations for which a 1961-1990 normal is available. The areal averages (Tables 2 and 3) and deciles are calculated from monthly analyses using a high-quality subset of the temperature network.

Maximum temperatures averaged over Australia for winter were 1.64°C above the long-term average, well above the previous record of +1.41°C set in 2002. Queensland (+2.33°C) and the Northern Territory (+2.04°C) also set winter records, by more than a degree in Queensland's case. All other States also ranked in the top ten (of the 60 years in the data-set), with South Australia and New South Wales second highest, and Victoria third highest. Overnight minimum temperatures (nationally 1.02°C above average) were less extreme, but still ranked as the fifth highest on record, with State records being set in South Australia (+1.83°C) and Tasmania (+1.42°C). Combining maximum and minimum temperatures, the national seasonal mean was 1.33°C above average, just 0.01°C short of the record set in 1996. The southeast was particularly warm, with State record winter mean temperatures being set in New South Wales (+1.48°C, previous highest +1.48°C), Victoria (+1.00°C, previous highest +0.93°C) and South Australia (+1.76°C, previous highest +1.36°C).

Maximum temperatures were above average across almost the whole of the country, the exceptions being a few places in Western Australia. Apart from some parts of the south and west, maxima were at least 1°C above average reaching 2–3°C above average over a large area encompassing the southern half of the Northern Territory, the southern half of Queensland away from the coast, northeastern South Australia and northwestern New South Wales. Record high values covered a substantial area (26.8 per cent of the country), and included parts of the Northern Territory and all States apart from Tasmania (60 per cent of Queensland, 40.7 per cent

Fig. 17 Winter 2009 temperature anomalies (°C) for Australia: anomalies based on 1961-1990 mean. Left: Maximum temperature anomalies, right: Minimum temperature anomalies.

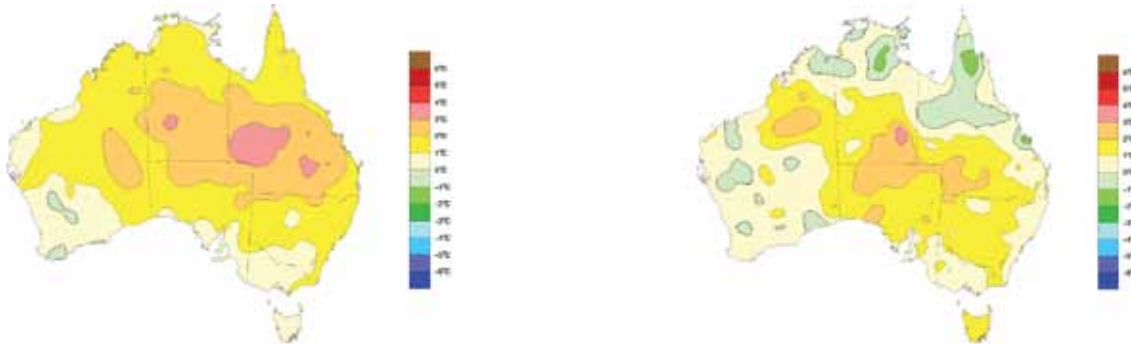
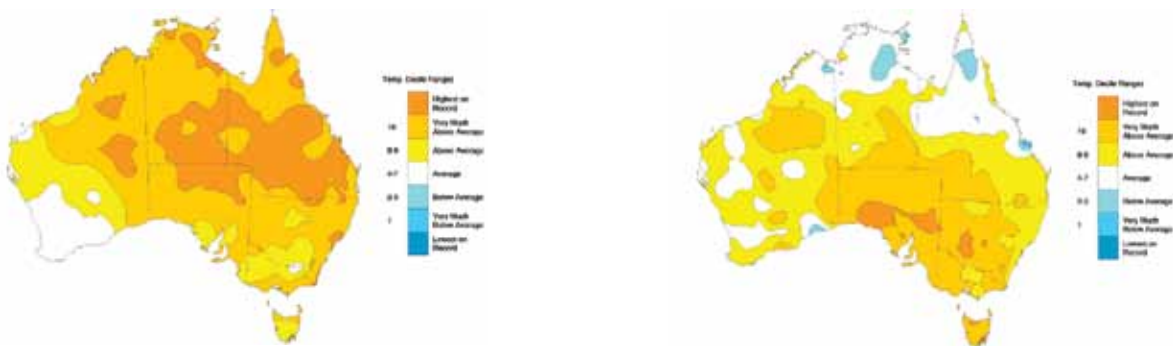


Fig. 18 Winter 2009 temperature deciles for Australia. Decile ranges are based on grid-point values over the winters 1911-2009. Left: Maximum temperature deciles, right: Minimum temperature deciles.

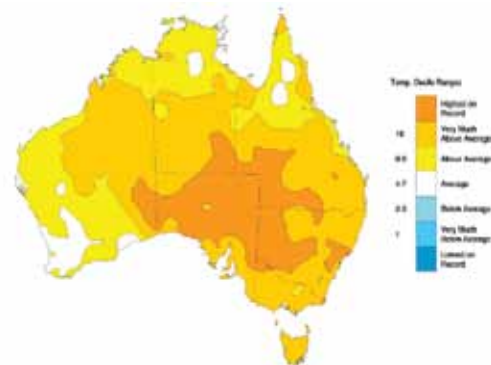


of the Northern Territory, 25.3 per cent of South Australia). A significant part of the country (77.7 per cent) saw very much above average (decile 10) seasonal maximum temperatures, comprising 100 per cent of Queensland, 98.7 per cent of the Northern Territory, 88.9 per cent of South Australia and 77.4 per cent of New South Wales.

Winter minimum temperatures were characterised by a large area of positive anomalies stretching from the north-west across the centre down into the southeastern States, with scattered smaller areas of negative anomalies in Western Australia, northern parts of the Northern Territory and Queensland around to central coastal Queensland. Positive anomalies reached +3°C in the southeast of the Northern Territory, while +1°C anomalies covered all of Tasmania. Record minimum temperatures for the season were observed over 18.4 per cent of South Australia, 6.2 per cent of New South Wales and 11.7 per cent of Tasmania.

Winter mean temperature anomalies (not shown) were positive across almost the entire country, the exceptions being two small regions, one on Cape York Peninsula, the

Fig.19 Winter 2009 mean temperature deciles for Australia. Decile ranges are based on grid-point values for winters 1911-2009.



other in southern Western Australia. Seasonal record mean temperatures (Fig. 19) occurred over 21.2 per cent of the country, comprising 72.3 per cent of South Australia, 44.7 per cent of New South Wales and 18.1 per cent of Queensland.

Table 2. Summary of seasonal maximum temperature ranks and extremes, on a national and State basis.

	<i>Highest seasonal mean (°C)</i>	<i>Lowest seasonal mean (°C)</i>	<i>Highest daily recording (°C)</i>	<i>Lowest daily recording (°C)</i>	<i>Anomaly of area-averaged mean (°C) (AAM)</i>	<i>Rank of AAM*</i>
Australia	34.1 at Noonamah (NT)	0.2 at Mount Hotham (Vic)	39.7 at Wyndham (WA), 31 August	-6.4 at Thredbo Top Station (NSW), 10 June	+1.64	60
WA	33.6 at Kalumburu	14.4 at Rocky Gully	39.7 at Wyndham, 31 August	8.8 at Shannon, 29 June	+1.00	54
NT	34.1 at Noonamah	22.5 at Kulgera	39.1 at Bradshaw, 31 August	10.1 at Kulgera, 1 June	+2.04	60
SA	22.5 at Oodnadatta	10.7 at Mount Lofty	35.3 at Oodnadatta, 15 August	6.8 at Mount Lofty, 14 July	+1.69	59
QLD	32.5 at Scherger	16.4 at Applethorpe	38.5 at Bedourie, 29 August	8.6 at Applethorpe, 16 July	+2.33	60
NSW	22.6 at Lismore	0.5 at Thredbo Top Station	37.8 at Mungindi, 24 August	-6.4 at Thredbo Top Station, 10 June	+1.61	59
VIC	17.3 at Mildura	0.2 at Mount Hotham	27.6 at Mildura, 15 August	-5.7 at Mount Hotham, 10 June	+1.12	58
TAS	14.7 at Scamander	3.3 at Mount Wellington	20.8 at Dover and Bushy Park, 15 August	-2.3 at Mount Wellington, 6 July	+0.70	52

* The temperature ranks go from 1 (lowest) to 60 (highest) and are calculated over the years 1950 to 2009 inclusive. Multiple ranks indicate the presence of tied values within the time series.

Table 3. Summary of seasonal minimum temperature ranks and extremes, on a national and State basis.

	<i>Highest seasonal mean (°C)</i>	<i>Lowest seasonal mean (°C)</i>	<i>Highest daily recording (°C)</i>	<i>Lowest daily recording (°C)</i>	<i>Anomaly of area-averaged mean (°C) (AAM)</i>	<i>Rank of AAM*</i>
Australia	23.7 at Troughton Island (WA)	-3.9 at Thredbo Top Station (NSW)	26.3 at Troughton Island (WA), 31 August	-14.9 at Charlotte Pass (NSW), 16 July	+1.02	56
WA	23.7 at Troughton Island	4.6 at Southern Cross	26.3 at Troughton Island, 31 August	-3.6 at Eyre, 26 August	+0.75	53
NT	23.6 at McCluer Island	6.3 at Arltunga	25.9 at Dum in Mirrie, 31 August	-1.7 at Arltunga, 5 August	+1.12	54
SA	12.3 at Neptune Island	4.1 at Yongala	21.5 at Moomba, 29 August	-4.7 at Yunta, 7 July	+1.83	60
QLD	24.2 at Coconut Island	2.8 at Stanthorpe	26.3 at Coconut Island, 2 June	-5.2 at Oakey, 12 June	+0.72	47
NSW	13.2 at Cape Byron	-3.9 at Thredbo Top Station	23.3 at Lismore, 25 August	-14.9 at Charlotte Pass, 16 July	+1.34	57
VIC	9.8 at Wilsons Promontory	-3.3 at Mount Hotham	15.2 at Orbost, 7 August	-7.9 at Mount Hotham, 11 June	+0.88	57
TAS	8.7 at Cape Grim	-1.1 at Mount Wellington	13.6 at Flinders Island, 4 June	-8.6 at Liawenee, 17 July	+1.42	60

* The temperature ranks go from 1 (lowest) to 60 (highest) and are calculated over the years 1950 to 2009 inclusive. Multiple ranks indicate the presence of tied values within the time series.

References

- Chandler, E. 2009. Seasonal climate summary southern hemisphere (autumn 2009). *Aust. Met. Oceanogr. J.*, 58, 285-95.
- Climate Diagnostics Center 2009a. Numerical values of the MEI time series since 1950. <http://www.cdc.noaa.gov/people/klaus.wolter/MEI/table.html>.
- Climate Diagnostics Center 2009b. Historical ranks of the MEI. <http://www.cdc.noaa.gov/people/klaus.wolter/MEI/rank.html>
- Climate Prediction Center 2009. Monthly mean AAO index since January 1979. http://www.cpc.noaa.gov/products/precip/CWlink/daily_ao_index/ao/ao.shtml.
- Donald, A., Meinke, H., Power, B., Wheeler, M. and Ribbe, J. 2004. Forecasting with the Madden-Julian Oscillation and the applications for risk management. In: *4th International Crop Science Congress*, 26 September - 01 October 2004, Brisbane, Australia.
- Kanamitsu, M., Ebisuzaki, W., Woollen, J., Yang, S.-K., Hnilo, J.J., Fiorino, M. and Potter, G.L. 2002. NCEP-DOE AMIP-II Reanalysis (R-2). *Bull. Am. Met. Soc.* 83, 1631-43.
- Reynolds, R.W., Rayner, N.A., Smith, T.M., Stokes, D.C. and Wang, W. 2002. An improved in situ and satellite SST analysis for climate. *Jnl Climate*, 15, 1609-25.
- Saji, N.H., Goswami, B.N., Vinayachandran, P.N. and Yamagata, T. 1999. A dipole mode in the tropical Indian Ocean. *Nature*, 401, 360-3.
- Troup, A.J. 1965. The Southern Oscillation. *Q. Jl R. Met. Soc.*, 91, 490-506.
- Vincent, D.G., Fink, A., Schrage, J.M. and Speth, P. 1998. High-and-low frequency intraseasonal variance of OLR on annual and ENSO timescales. *Jnl Climate*, 11, 968-86.
- Wheeler, M.C. and Hendon, H.H. 2004. An all-season real-time multivariate MJO index: Development of an index for monitoring and prediction. *Mon. Weath. Rev.*, 132, 1917-32.
- Wolter, K. and Timlin, M.S. 1993. Monitoring ENSO in COADS with a seasonally adjusted principal component index. *Proc. of the 17th Climate Diagnostics Workshop*, Norman, OK, NOAA/NMC/CAC, NSSL, Oklahoma Clim. Survey, CIMMS and the School of Meteorology, Univ. of Oklahoma, 52-7.
- Wolter, K. and Timlin, M.S. 1998. Measuring the strength of ENSO – how does 1997/98 rank? *Weather*, 53, 315-24.

